Liquefaction of Fir Sawdust in Supercritical Ethanol with Dissolved Phosphotungstic Acid

Changwei Zeng, Huaiyu Zheng, Jianhua Lv, Xuerong Chen, and Biao Huang *

An environmentally benign approach is put forward with the focus on directly liquefying and depolymerizing *Cunninghamia lanceolata* (Lamb.) Hook. (Chinese fir) sawdust into ethyl levulinate (EL) under supercritical ethanol (scEtOH) conditions by using phosphotungstic acid (PTA) as a catalyst. The effects of parameters such as catalyst dosage, temperature, and reaction time on alcoholysis yield were investigated. The experimental results show that the biomass alcoholysis yield reached 95.35% with 0.5 g PTA as a catalyst at 260 °C for 30 min. Alcoholysis yield and quantitative content of EL depended on the catalyst. The light bio-oil was primarily composed of phenols, aldehydes, ketones, and esters. A high quantitative content of EL up to 20.82% (A_R, Relative abundance) was achieved, compared to 0.73% A_R when PTA was not added. Hence, scEtOH with dissolved PTA may offer novel media for both chemical reactions and biomass conversion technology as a replacement for environmentally undesirable organic solvents.

Keywords: Phosphotungstic acid; Supercritical ethanol; Liquefaction; Ethyl levulinate; Sawdust

*Contact information: College of Material Engineering, Fujian Agriculture and Forestry University, Fuzhou 350002, China; *Corresponding author: fjhuangbiao@hotmail.com*

INTRODUCTION

Developing new methods to convert biomass into fuels and high-value-added chemicals can reduce our dependence on fossil fuels. In recent years there has been much research on thermo-chemical conversion of biomass into bio-fuels by catalytic hydrolysis technology. This effort has been motivated by the socio-economic advantages of the process as well as the fact that it is an efficient conversion method compared to other conversion technologies. However, some drawbacks also arise, which involve oxidation, corrosion, environmental contamination, and high costs. Therefore, exploring an efficient and environmentally-friendly method and catalyst has been imperative.

With the development of supercritical fluid technology, much work has been devoted to discovering its potential advantages for biomass conversion. In addition to supercritical water (Sawai *et al.* 2013), supercritical organic solvents including methanol (Saka and Kusdiana 2001; Imahara *et al.* 2009), ethanol (Warabi *et al.* 2004; Yamazaki *et al.* 2006), acetone (Jin *et al.* 2014) and phenol (Mishra and Saka 2011) have been applied to the liquefaction of biomass. In particular, compared with other liquefaction solvents, ethanol is regarded as the most promising for liquefaction, not only because of its high efficiency, but also because of its renewability and the fact that there are numerous sources (Xu and Etcheverry 2008).

Ethyl levulinate (EL), a food additive approved by the Food and Drug Administration, is common in perfumes and candles. EL has greater miscibility with petrochemical fuels than either soy diesel or ethanol. EL can be used as a platform

chemical for the production of a wide range of value-added products. In general, EL can be obtained by esterification of levulinic acid and alcohols (Fernandes *et al.* 2012; Pasquale *et al.* 2012).

Heteropolyacids (HPAs) are some of the most attractive catalysts because they are commercially available, easy to handle, and environmentally-friendly with remarkably low toxicity and economy. Phosphotungstic acid (PTA), the strongest heteropolyacid, is known as a highly efficient green catalyst (Ninomiya *et al.* 2011). Some literature has reported the esterification of fatty acids into biodiesel by using PTA-supported carriers such as activated carbon, SBA-15 (Tropecêlo *et al.* 2010; Brahmkhatri and Patel 2012), mesoporous silica (Patel and Brahmkhatri 2013), and zirconia (Oliveira *et al.* 2010).

It is well known that the thermo-chemical conversion of biomass by catalytic hydrolysis is a heterogeneous reaction because of the solid particle form of the biomass raw material. If the form of the catalyst is also solid, with both the raw material and the catalyst in the solid phase, then the diffusivity, heat transfer, selectivity, and active site of the catalyst might be a problem for the reaction system.

However, PTA can be dissolved in alcohols and can be easily separated by organic solvents such as diethyl ether. Therefore, in combination with the advantages of scEtOH and PTA, the application of scEtOH with dissolved PTA as an enhanced medium and catalyst could lead to many benefits for lignocellulosic biomass liquefaction.

Based on the combined advantages of scEtOH and PTA, the application of scEtOH with dissolved PTA as an enhanced medium and catalyst is adopted in this study. To the best of our knowledge, few studies have been carried out to directly liquefy and depolymerize lignocellulosic biomass into value-added chemicals such as EL by this method. To understand the role of liquefaction factors and PTA in the direct liquefaction of sawdust, the effects of reaction parameters including reaction time, temperature, and dosage of catalyst were investigated. In addition, the compositions of liquefaction products were analyzed by various characterization methods.

EXPERIMENTAL

Materials

Fir sawdust (Fuzhou, China) was ground to the range 0.25 to 0.42 mm. The sample was dried in an oven at 105 °C until it reached a constant weight. Typical biomass constituents of the dried fir sawdust, in terms of cellulose, hemi-cellulose and lignin, were analyzed according to the Chinese GB/T 2677 standard (Comprehensive Business Department of China Light Industry Council 2010) with the following results: cellulose content of 41.01%, hemicellulose content of 27.09%, and acid-insoluble lignin content of 30.24%. Chemical reagents such as ethanol, PTA, and n-hexane were of analytic grade and purchased from the Sinopharm Chemical Reagent Company (Shanghai, China). High-purity nitrogen (99.99% purity) was purchased from the Huaxinda Industrial Gas Company (Fuzhou, China).

Methods

The liquefaction of fir sawdust was performed in a 300-mL stainless-steel, magnetically stirred autoclave, into which a 1-g fir sawdust sample, 150 g of ethanol, and the desired amount of catalyst (PTA) were added. First, the autoclave was sealed and purged three times using high-purity nitrogen to replace the air within the reactor. Then,

the reactor was heated to the desired temperature at a heating rate of 5 °C/min and kept at that temperature for 10 to 50 min. After the reaction, the autoclave was quenched with a cooling pipe using external cool water and an industrial fan.

The experimental procedure is illustrated in Fig. 1. The gaseous fraction was evacuated after the reactor had been cooled to room temperature. The liquid and solid fractions were poured out from the autoclave, and the wall of the autoclave was rinsed several times with ethanol; then the liquid and solid products were filtrated through a Buchner funnel with a pre-weighed filter paper. The filter cake (solid residue, SR) was repeatedly rinsed with ethanol until the filtrate was transparent and colorless. The SR was extracted using water *via* a Soxhlet extractor for 24 h to remove residual PTA, dried at 105 °C in an oven until a constant weight was obtained, and then weighed to obtain the yield of SR. The filtrate was distilled with a rotary evaporator to remove the ethanol under vacuum at 70 °C. The resulting liquid phase product after the distillation was designated as bio-oil (BO). The SR yield, biomass alcoholysis yield, HBO ratio and LBO ratio were calculated according to Eqs. 1 and 2 as follows:

$$\text{SR yield (\%)} = \text{weight of SR/ weight of the dried fir sawdust} \times 100 \quad (1)$$

$$\text{Biomass alcoholysis yield (\%)} = 100\ \% - \text{SR yield} \quad (2)$$

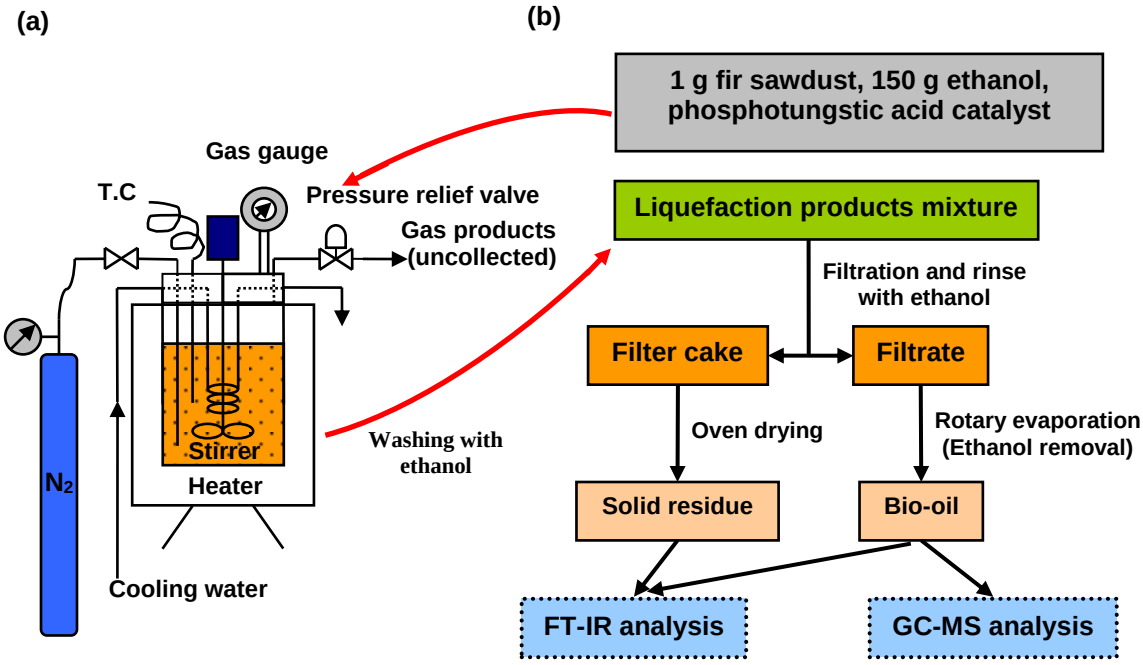

Fig. 1. The schematic diagram of (a) the autoclave and (b) procedure chart of the supercritical liquefaction of fir sawdust

The surface morphology analyses for SR obtained from liquefaction with and without PTA catalyst were performed by using a microscope (JEOL Model JSM-7500F, Japan). Thermogravimetric experiments of SR and sawdust were achieved using a NETZSCH STA 449 F3 Jupiter® (Germany) simultaneous thermal analyzer. The

temperature was increased from 25 to 800 °C at a rate of 10 °C/min with a 30 mL/min flow of N_2 as a carrier gas.

The fir sawdust and SR without Soxhlet extraction were completely mixed with potassium bromide at a mass ratio of 1:150. After this, they were ground in an agate mortar and compacted into a sheet by a hydraulic press at a pressure of approximately 20 MPa. The functional group information of the sample was characterized by FT-IR spectroscopy using a Nicolet 380 FT-IR spectrophotometer (Thermo Fisher Scientific, USA). FT-IR spectra were obtained in the 4000 to 400 cm^{-1} region, with a total of 32 replicate scans and a resolution of 4 cm^{-1} using OMNIC software (Thermo Fisher Scientific, USA) (Christensen *et al.* 2014; Lu *et al.* 2013).

The BO sample, after the ethanol removal process, was reprocessed by means of extraction with hexane and centrifuged at a desired rotating speed with a high-speed centrifuge. Subsequently, the BO sample was separated into a black viscous substance, which was specified as heavy bio-oil (HBO), and a dark brown immiscible liquid, which was designated as light bio-oil (LBO). HBO was analyzed by FT-IR spectra. The GC-MS analysis of LBO was performed using an Agilent 7890/5975C gas chromatography-mass spectrometer (USA) equipped with a neutral polar DB-17 m capillary column (30 m × 0.25 mm × 0.25 μm), utilizing helium as a carrier gas at a constant flow rate of 25 mL/min. The LBO sample of 1 μL was injected at a split ratio of 15:1 at 280 °C.

RESULTS AND DISCUSSION

The Effect of Main Process Parameters on Biomass Alcoholysis Yield

Temperature is an important parameter in supercritical ethanol liquefaction reactions. Figure 2(a) shows the effect of reaction temperature on biomass alcoholysis yield, in which the alcoholysis yield increased continuously from 78.70% to 95.35% as the reaction temperature increased from 180 to 260 °C, whereas alcoholysis yield rose slightly from 95.35% to 95.83% as the reaction temperature was extended beyond 260 °C. At low reaction temperature (from 180 to 200 °C), the alcoholysis yield increased slowly from 78.70% to 82.24%. This could be due to the fact that the fir sawdust did not fully react under subcritical ethanol conditions (Xu *et al.* 2014). However, the alcoholysis yield dramatically increased to 95.35% as the temperature approached 260 °C, beyond the critical conditions of ethanol, whose critical temperature and pressure are 242.8 °C and 6.36 MPa, respectively. The results indicated that the high diffusivity and solubility of ethanol favored the liquefaction of wood. In addition, compared with 260 °C, the conversion yield did not change noticeably when the temperature reached 280 °C, as raising the temperature could promote the decomposition of sawdust and the recondensation of the liquefaction intermediates simultaneously (Jin *et al.* 2011). Furthermore, the high conversion yield of 95.35% also suggested that the three major components, namely cellulose, hemicellulose, and lignin, were basically liquefied when compared to their total content of 98.34%. With economic benefits and energy consumption taken into consideration, 260 °C was selected as the optimal reaction temperature for fir sawdust.

The effect of the reaction time on biomass alcoholysis yield is shown in Fig. 2(b), in which the change of biomass alcoholysis yield over reaction time was investigated at a reaction temperature of 260 °C and catalyst dosage of 0.5 g. At first, the biomass alcoholysis yield increased from 92.52% with the reaction time of 10 min to 95.35% with

a reaction time of 30 min. However, the alcoholysis yield increased only slightly when the reaction time was extended beyond 30 min (95.38% with the reaction time of 40 min), which may be due to the saturation of the raw sawdust primary liquefaction when the reaction time was longer than 30 min. In addition, an increase of resistance time in the 40 to 50 min range resulted in a decrease in the alcoholysis yield from 95.38% to 92.31% because of the formation of residue caused by condensation and repolymerization (Li *et al.* 2009; Zhao *et al.* 2013). Thus, all the supercritical liquefaction of fir sawdust experiments were conducted with the reaction time of 30 min.

The effect of catalyst dosage on biomass alcoholysis yield is shown in Fig. 2(c), which presents the results obtained from the supercritical liquefaction operations with various catalyst dosages from 0 to 1.0 g at 260 °C for the resistance time of 30 min. The biomass alcoholysis yield rose dramatically and then tended to stay steady with catalyst dosage increasing. The increase in the biomass alcoholysis yield, from 58.89% without catalyst to 79.42% with 0.1 g of catalyst, indicates that PTA could distinctly enhance the biomass alcoholysis efficiency for supercritical liquefaction of fir sawdust. For a catalyst dosage greater than 0.5 g, there was no obvious promoting effect on the biomass alcoholysis yield, from 93.35% with 0.5 g of catalyst to 96.33% with 1.0 g of catalyst. Given that the excess catalyst may have possibly not been consumed, the residual PTA left in SR may result in the waste of the catalyst. Therefore, the most appropriate dosage of PTA was determined to be 0.5 g.

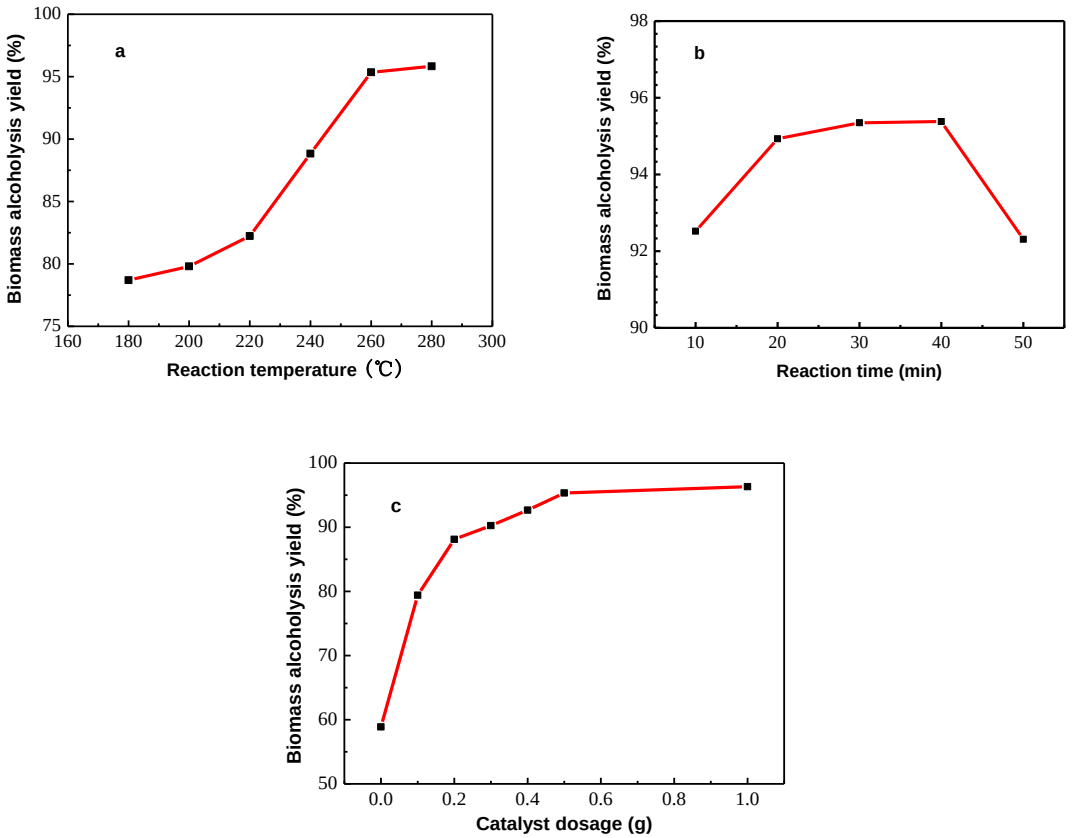

Fig. 2. Effect of (a) reaction temperature, (b) reaction time, and (c) dosage of catalyst on biomass alcoholysis yield

SEM Analysis

Figure 3 shows SEM images of SR obtained from liquefaction of fir sawdust with and without PTA catalyst. The SEM images show distinct differences in the morphology of SR. For the run without catalyst, the fiber cell wall of SR was not sufficiently cracked and still maintained the fiber structure. The formation of carbon spheres with a diameter of less than 1 μm was observed from the run with catalyst. This phenomenon could be explained by the increase in the biomass alcoholysis yield, from 58.89% without catalyst to 95.35% with 0.5 g PTA. On the other hand, the results also indicate that PTA could dramatically catalyze the formation of carbon spheres during the liquefaction process (Tekin *et al.* 2012).

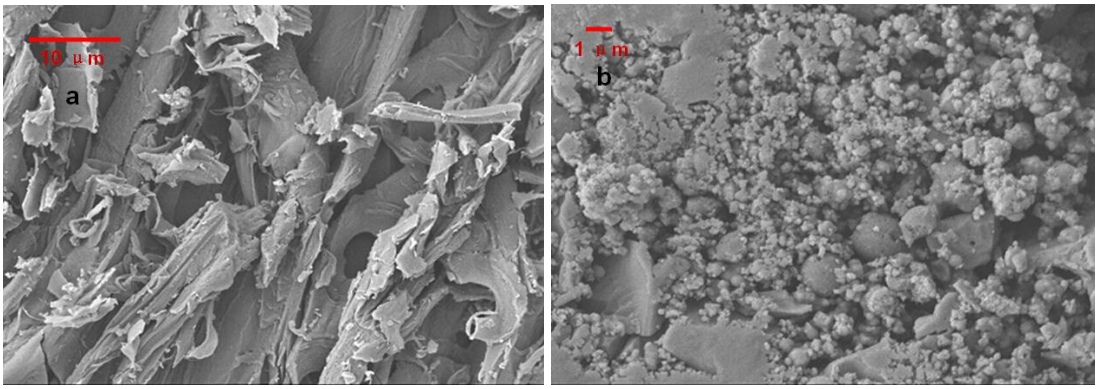

Fig. 3. SEM images of SR obtained from liquefaction of fir sawdust at 260 °C for 30 min (a) without and (b) with PTA catalyst

FT-IR Analysis

Figure 4(a) shows the FT-IR spectra of fir sawdust. Generally, the characteristic absorption peaks of cellulose are at 2907, 1369, 1023, and 896 cm^{-1} (Schwanninger *et al.* 2004). Lignin shows distinct bands at 1599, 1506, 1422, and 814 cm^{-1} (Lu *et al.* 2014). The broad absorption peak near 3392 cm^{-1} may be due to O-H stretching originating from the presence of cellulose and/or polysaccharide compounds (hemicellulose) (Chen *et al.* 2012). The strong absorbance at 2915 cm^{-1}, attributed to the C-H stretching vibrations, indicates the presence of methyl and methylene groups (Brand *et al.* 2013). The typical carbonyl group (C=O) stretching vibrations at 1732 cm^{-1} in the sample show the characteristic absorption peak of hemicellulose (Meryemoğlu *et al*. 2014). Aromatic skeletal vibrations originating from lignin are confirmed by aromatic C=C stretching at 1614, 1510, and 1425 cm^{-1} (Aysu and Küçük 2013). In contrast, compared with the spectrum of fir sawdust, there is a marked difference in the FT-IR spectra of SR.

As is shown in Fig. 4(b), the four characteristic bands for the Keggin structure of PTA in SR appear at 1079, 984, 892, and 811 cm^{-1} and are assigned to the vibrations of asymmetric P-O at the central tetrahedral, terminal asymmetric oxygen ($W = O_d$), corner shared asymmetric oxygen ($W\text{-}O_b\text{-}W$), and edge-shared oxygen ($W\text{-}O_c\text{-}W$), respectively (Gong *et al.* 2014). As for the SR sample, the four Keggin-structured bands in the spectra indicate that the PTA in SR still retained the Keggin structure. This phenomenon can be explained as being a result of the high thermal stability of PTA anions, which indicates that PTA can be effectively reused for reprocessing SR.

The broad bands near 3392 and 2915 cm^{-1} were noticeably reduced. In addition, the disappearance of the absorption peak at 1732 cm^{-1} suggests that the hemicellulose in

fir sawdust was completely liquefied. Intensity peaks can be observed near 2860 cm^{-1}, which is the characteristic absorption peak of methoxyl groups in lignin. From the above results it can be inferred that cellulose and hemicellulose are easier to liquefy than lignin, especially hemicellulose. Holocellulose depolymerization can be rationalized as a combined effect of the much higher dielectric constant of supercritical ethanol (in contrast with the dielectric constant of ethanol in the liquid state) and the ability of ethanol to undergo autoprotolysis (Rataboul and Essayem 2011).

The band at 1700 cm^{-1} can be attributed to aromatic conjugated C=O stretching vibrations. The skeletal vibration bands of benzene rings can be observed at 1600 and 1420 cm^{-1}, while an absorption peak appears at 1510 cm^{-1}. These phenomena indicate that compounds with benzene ring structures are present in SR. These compounds are primarily the lignin derivatives obtained from liquefaction products, which are different from the lignin structure of raw sawdust (Xu *et al.* 2012). As expected, the lignin derivatives existing in SR show that the lignin in sawdust might not be entirely liquefied and might generate the repolymerization derivatives of depolymerized lignin.

Figures 4(c) and (d) show the FT-IR spectra of HBO obtained from liquefaction without catalyst and with PTA catalyst, respectively. The intense broad bands at 1079, 981, 894, and 813 cm^{-1} in Fig. 4(d) can be assigned to the four characteristic bands for the Keggin structure of PTA (Gong *et al.* 2014). The intense band at 1713 cm^{-1} originating from the presence of C=O groups in HBO obtained with PTA catalyst, which are not present in HBO obtained without catalyst, indicates that PTA can promote the formation of ketones, aldehydes, and carboxylic acids. The peaks observed at 1599, 1452, and 1410 cm^{-1} can be attributed to aromatic rings, which are related to lignin (Lu *et al.* 2014). The results indicate that HBO could be obtained from lignin by a certain type of destruction, regardless of whether PTA is added as a catalyst or not.

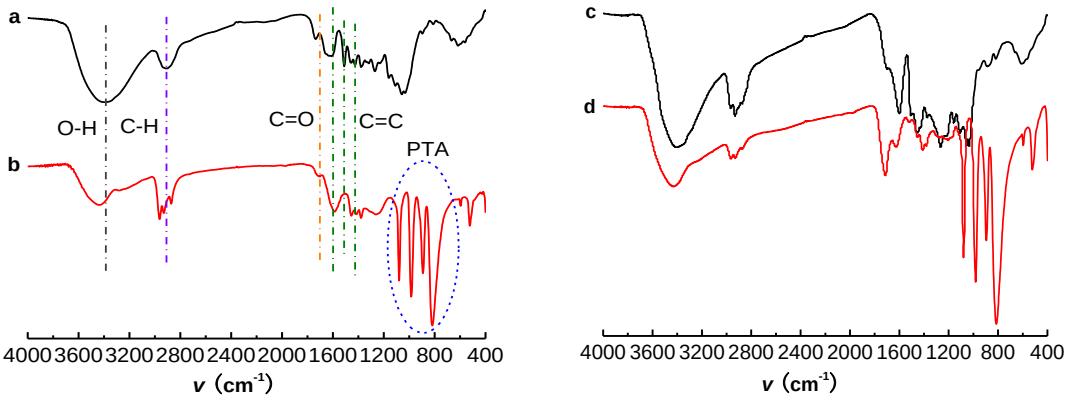

Fig. 4. FT-IR spectra of (a) fir sawdust; (b) solid residue (SR); (c) HBO obtained by liquefaction without catalyst, and (d) with 0.5 g of PTA catalyst fixed at 260 °C for 30 min

TG and DTG Analysis

The thermal degradation behavior of fir sawdust and SR without Soxhlet extraction was conducted using TG and DTG analysis (Fig. 5). The TG and DTG curves of fir sawdust and SR are distinctly different because of their different compositions, as determined by the FT-IR analysis. The main degradation temperature of fir sawdust was from 214 to 526 °C and lower than 134 °C, while that of SR was from 318 to 521 °C and

above 521 °C. In the range of 25 to 134 °C, the weight loss of fir sawdust was 9%, which was attributed to the loss of hydroxyl bonded water.

Hemicellulose and cellulose decomposition peaks were observed between 214 and 370 °C (Chen and Kuo 2010). In Fig. 5(b), the broad peak of weight loss was between 300 and 370 °C, with a maximum rate of weight loss occurring at 359 °C, possibly contributed by the simultaneous thermal decomposition of hemicellulose and cellulose (Chan *et al.* 2014). For the SR, a slight decrease in weight occurred between 318 and 521 °C, which corresponded to the decomposition of lignin and the crystal water in the residual dystectic PTA (Ninomiya *et al.* 2011). At temperatures higher than 521 °C, the rate of weight loss increased, which is attributed to the decomposition of lignin and the residual PTA (Idris *et al.* 2010; Ninomiya *et al.* 2011). These phenomena indicate that the SR was composed of lignin and PTA, consistent with the results of the FT-IR analysis.

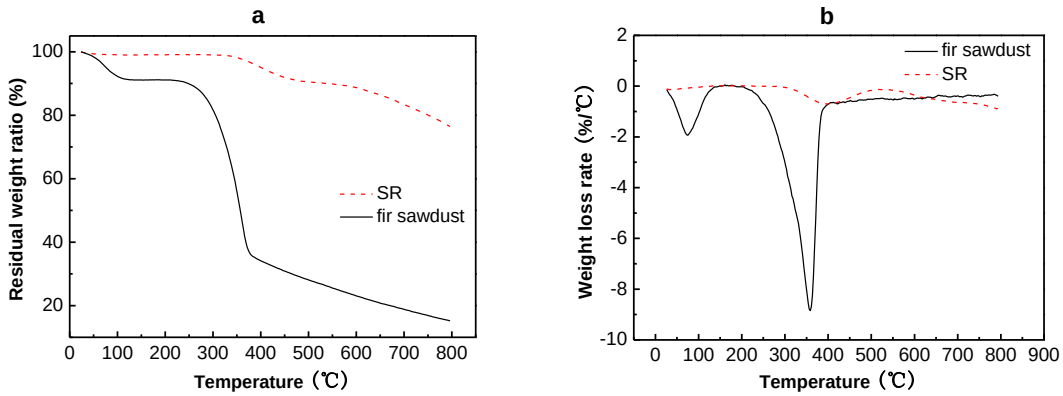

Fig. 5. Comparison of (a) TG and (b) DTG curves for fir sawdust and SR

GC-MS Analysis

The major compounds of LBO were analyzed using GC-MS to obtain more detailed information on the components. The quantitative content of the main compounds in LBO was determined using the area normalization method. GC-MS analysis results of LBO obtained from liquefaction without catalyst but with PTA are shown in Tables 1 and 2. It should be noted that these findings represent only a part of the LBO compounds. Other compounds are difficult to identify because of their much lower match degree with the mass spectral library.

It is clear that the composition of LBO was prominently affected by the PTA catalyst; 25 main compounds were identified in LBO without catalyst and only 17 kinds were found in a PTA catalysis run. The distribution of the main composition in LBO is illustrated in Fig. 6. It was found that LBO obtained without catalyst involved more phenols, whereas there were more esters in LBO with a PTA catalyst. The quantitative content of alkenes and phenols decreased as esters increased when PTA was added as a catalyst, which indicated that PTA promoted the degradation and esterification of macromolecules. With the addition of PTA in the reaction, the quantitative content of aldehydes decreased, in contrast to the increased content of ketones, because of the enhancement of oxidation in this reaction system.

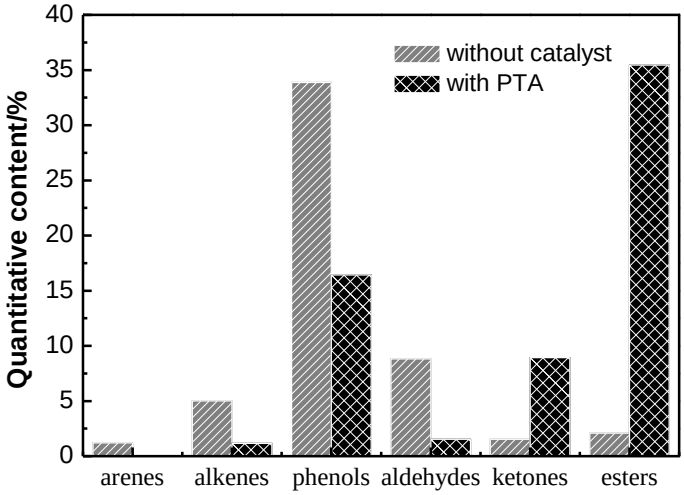

Fig. 6. The quantitative content distribution of compounds in LBO obtained from liquefaction without catalyst and with PTA catalyst

As can be inferred from Tables 1 and 2, a high quantitative content of EL, up to 20.82% relative abundance (A_R), was achieved, compared to the 0.73% A_R achieved when PTA was not used as catalyst.

Table 1. Major Compounds Identified in LBO Produced at 260 °C and 30 min without Catalyst

Peak NO.	Retention time/min	Compound	Relative abundance */%
1	5.366	p-Xylene	1.21
2	8.834	Ethoxyacetaldehyde diethylacetal	6.63
3	12.497	2-hydroxy-3-methyl-2-Cyclopenten-1-one	0.43
4	13.642	Ethyl levulinate	0.73
5	14.231	Guaiacol	1.13
6	17.04	2-Methoxy-5-methylphenol	0.67
7	19.844	α-Cedrene	4.38
8	20.314	β-Cedrene	0.64
9	20.827	2-Methoxy-4-vinylphenol	7.21
10	21.594	3-Allyl-6-methoxyphenol	3.5
11	23.171	Eugenol	1.07
12	24.343	trans-Isoeugenol	19.16
13	24.662	Vanillin	1.36
14	24.851	4-(Ethoxymethyl)-2-methoxyphenol,	1.15
15	26.726	Apocynin	1.1
16	28.346	Ethyl 4-hydroxy-3-methoxybenzoate	1.36
17	30.102	3,5-Di-tert-butyl-4-hydroxybenzaldehyde	0.82
Total			52.55
* This parameter is relative to the total abundance of all compositions detected by GC-MS			

Table 2. Major Compounds Identified in LBO Produced at 260 °C and 30 min with 0.5 g PTA

Peak No.	Retention time/min	Compound	Relative abundance */%
1	13.782	3-Methyl-1,2-cyclopentanedione	1.63
2	14.91	Ethyl levulinate	20.82
3	15.432	Ethyl valerate	0.69
4	15.563	Guaiacol	3.78
5	16.898	2-Ethoxyphenol	0.72
6	17.064	4,4-Dimethyl-1,3-cyclohexanedione	3.06
7	17.385	Tert butyl ethyl succinate	1.98
8	17.587	Diethyl succinate	0.75
9	18.335	2-Methoxy-4-methylphenol	0.51
10	18.946	1-Ethoxy-4-methoxy-benzene	0.96
11	19.534	Diisopentyl succinate	1.12
12	20.578	4-Ethyl-2-methoxyphenol	1.81
13	21.219	α-Cedrene	1.17
14	22.721	2-Methoxy-4-n-propylphenol	1.93
15	25.783	4'-Ethoxyacetophenone	1.16
16	26.033	Isovanilin	1.53
17	27.807	3,5-Di-tert-butylphenol	1.30
18	28.152	Methyl 4-hydroxy-3-methoxyphenylacetate	5.18
19	29.713	Ethyl 4-hydroxy-3-methoxybenzoate	3.31
20	30.282	2-Pentyl-3-methyl- -2-cyclopenten-1-one	3.08
21	30.941	2,4,6-Triisopropylphenol	2.33
22	31.066	2,6-Di-tert-butyl-4-methylphenol	1.37
23	31.481	2,6-Di-tert-butyl-4-ethylphenol	3.01
24	33.743	Palmitic acid ethyl ester	0.45
25	45.53	Diisopentyl phthalate	1.15
Total			64.79
* This parameter is relative to the total abundance of all compositions detected by GC-MS			

It is clear that EL was the major compound identified in LBO obtained with a PTA catalyst, while trans-isoeugenol was the largest content compound in LBO obtained without catalyst. EL represented the largest portion identified in LBO produced from the esterification reactions of ethanol and levulinic acid obtained from the hydrolyzation of 5-hydroxymethul furfural in the decomposition products of cellulose or hemicellulose in ethanol with PTA (Huang *et al.* 2013). Methyl 4-hydroxy-3-methoxyphenylacetate and ethyl 4-hydroxy-3-methoxybenzoate can be obtained from the esterification of the degradation fragments of lignin (Li *et al.* 2009). Phenols such as 2-methoxy-4-vinylphenol, eugenol, guaiacol, 2-methoxy-4-n-propylphenol, 4-ethyl-2-methoxyphenol, and 2-methoxy-4-methylphenol were undoubtedly derived from the degradation of sawdust. This conforms to the conclusion that softwood lignin contains guaiacyl propane units (Brand *et al.* 2013). In addition, the benzene ring structure of degradation products may have the potential to be used in the synthesis of phenolic resin or other new functional materials (Xu *et al.* 2012).

CONCLUSIONS

1. The application of scEtOH with dissolved PTA as an enhanced medium and catalyst was adopted for liquefaction and depolymerization of Chinese fir sawdust into value-added chemicals. The results show that PTA had a remarkable effect on the quantitative content of EL.
2. The optimum reaction conditions for catalytic liquefaction were 260 °C, with a reaction time of 30 min and 150 g of ethanol as solvent, which could achieve the highest alcoholysis yield of 95.35%.
3. Based on the FT-IR and TG analyses, the SR was primarily composed of PTA catalyst and lignin derivatives. Meanwhile, GC-MS results show that the LBO was primarily composed of phenols, esters, aldehydes, ketones, and alkenes. Additionally, the phenols originated from the degradation of lignin in sawdust, while the increased content of esters in the absence of added catalyst was attributed to the esterification of acids obtained from decomposition of the main compounds in sawdust.
4. In particular, the high quantitative content of EL obtained by the esterification of levulinic acid degraded from cellulose and hemicellulose in scEtOH with PTA as catalyst suggests that PTA could play a key role in promoting the liquefaction of biomass and producing EL from fir sawdust in scEtOH.

ACKNOWLEDGMENTS

We appreciate the generous financial support of the Special Scientific Research Fund for Public Service Sectors of Forestry (Grant No. 201504603) and the National Natural Science Foundation of China (Grant No. 31370560, 31170520).

REFERENCES CITED

Aysu, T., and Küçük, M. M. (2013). "Liquefaction of giant fennel (*Ferula orientalis* L.) in supercritical organic solvents: Effects of liquefaction parameters on product yields and character," *The Journal of Supercritical Fluids* 83, 104-123. DOI: 10.1016/j.supflu.2013.09.001

Brahmkhatri, V. and Patel, A. (2012). "An efficient green catalyst comprising 12-tungstophosphoric acid and MCM-41: Synthesis characterization and diesterification of succinic acid, a potential bio-platform molecule," *Green Chemistry Letters and Reviews* 5(2), 161-171. DOI: 10.1080/17518253.2011.607471

Brand, S., Susanti, R. F., Kim, S. K., Lee, H.-S., Kim, J., and Sang, B.-I. (2013). "Supercritical ethanol as an enhanced medium for lignocellulosic biomass liquefaction: Influence of physical process parameters," *Energy* 59, 173-182. DOI: 10.1016/j.energy.2013.06.049

Chan, Y. H., Yusup, S., Quitain, A. T., Uemura, Y., and Sasaki, M. (2014). "Bio-oil production from oil palm biomass *via* subcritical and supercritical hydrothermal liquefaction," *The Journal of Supercritical Fluids* 95, 407-412. DOI: 10.1016/j.supflu.2014.10.014

Chen, W.-H., and Kuo, P.-C. (2010). "A study on torrefaction of various biomass materials and its impact on lignocellulosic structure simulated by a thermogravimetry," *Energy* 35(6), 2580-2586. DOI: 10.1016/j.energy.2010.02.054

Chen, Y., Wu, Y., Zhang, P., Hua, D., Yang, M., Li, C., Chen, Z., and Liu, J. (2012). "Direct liquefaction of *Dunaliella tertiolecta* for bio-oil in sub/supercritical ethanol–water," *Bioresource Technology* 124, 190-198. DOI: 10.1016/j.biortech.2012.08.013

Christensen, P. R., Mørup, A. J., Mamakhel, A., Glasius, M., Becker, J., and Iversen, B. B. (2014). "Effects of heterogeneous catalyst in hydrothermal liquefaction of dried distillers grains with solubles," *Fuel* 123, 158-166. DOI: 10.1016/j.fuel.2014.01.037

Comprehensive Business Department of China Light Industry Council (2010). "China light industry standard assembly: paper (I)," Standards Press of China, Beijing 464-482.

Fernandes, D., Rocha, A., Mai, E., Mota, C. J., and da Silva, V. T. (2012). "Levulinic acid esterification with ethanol to ethyl levulinate production over solid acid catalysts," *Applied Catalysis A: General* 425, 199-204. DOI: 10.1016/j.apcata.2012.03.020

Gong, S.-W., Lu, J., Wang, H.-H., Liu, L.-J., and Zhang, Q. (2014). "Biodiesel production via esterification of oleic acid catalyzed by picolinic acid modified 12-tungstophosphoric acid," *Applied Energy* 134, 283-289. DOI: 10.1016/j.apenergy.2014.07.099

Huang, H.-J., Yuan, X.-Z., Zeng, G.-M., Liu, Y., Li, H., Yin, J., and Wang, X.-L. (2013). "Thermochemical liquefaction of rice husk for bio-oil production with sub-and supercritical ethanol as solvent," *Journal of Analytical and Applied Pyrolysis* 102, 60-67. DOI: 10.1016/j.jaap.2013.04.002

Idris, S. S., Rahman, N. A., Ismail, K., Alias, A. B., Rashid, Z. A., and Aris, M. J. (2010). "Investigation on thermochemical behaviour of low rank Malaysian coal, oil palm biomass and their blends during pyrolysis via thermogravimetric analysis (TGA)," *Bioresource Technology* 101(12), 4584-4592. DOI: 10.1016/j.biortech.2010.01.059

Imahara, H., Xin, J., and Saka, S. (2009). "Effect of CO_2/N_2 addition to supercritical methanol on reactivities and fuel qualities in biodiesel production," *Fuel* 88(7), 1329-1332. DOI: 10.1016/j.fuel.2009.01.002

Jin, Y., Ruan, X., Cheng, X., and Lü, Q. (2011). "Liquefaction of lignin by polyethyleneglycol and glycerol," *Bioresource Technology* 102(3), 3581-3583. DOI: 10.1016/j.biortech.2010.10.050

Jin, B., Duan, P., Zhang, C., Xu, Y., Zhang, L., and Wang, F. (2014). "Non-catalytic liquefaction of microalgae in sub-and supercritical acetone," *Chemical Engineering Journal* 254, 384-392. DOI: 10.1016/j.cej.2014.05.137

Li, H., Yuan, X., Zeng, G., Tong, J., Yan, Y., Cao, H., Wang, L., Cheng, M., Zhang, J., and Yang, D. (2009). "Liquefaction of rice straw in sub-and supercritical 1,4-dioxane–water mixture," *Fuel Processing Technology* 90(5), 657-663. DOI: 10.1016/j.fuproc.2008.12.003

Lu, Z., Zheng, H., Fan, L., Liao, Y., Ding, B., and Huang, B. (2013). "Liquefaction of sawdust in 1-octanol using acidic ionic liquids as catalyst," *Bioresource Technology* 142, 579-584. DOI: 10.1016/j.biortech.2013.05.091

Lu, J., Li, X., Yang, R., Zhao, J., Liu, Y., and Qu, Y. (2014). "Liquefaction of fermentation residue of reed-and corn stover-pretreated with liquid hot water in the presence of ethanol with aluminum chloride as the catalyst," *Chemical Engineering Journal* 247, 142-151. DOI: 10.1016/j.cej.2014.02.094

Meryemoğlu, B., Hasanoğlu, A., Irmak, S., and Erbatur, O. (2014). "Biofuel production by liquefaction of kenaf (*Hibiscus cannabinus* L.) biomass," *Bioresource Technology* 151, 278-283. DOI: 10.1016/j.biortech.2013.10.085

Mishra, G., and Saka, S. (2011). "Kinetic behavior of liquefaction of Japanese beech in subcritical phenol," *Bioresource Technology* 102(23), 10946-10950. DOI: 10.1016/j.biortech.2011.08.126

Ninomiya, W., Sadakane, M., Ichi, Y., Yasukawa, T., Ooyachi, K., Sano, T., and Ueda, W. (2011). "Influence of structural differences and acidic properties of phosphotungstic acids on their catalytic performance for acylation of pyruvate ester to α-acyloxyacrylate ester," *Catalysis Today* 164(1), 107-111. DOI: 10.1016/j.cattod.2010.10.047

Oliveira, C. F., Dezaneti, L. M., Garcia, F. A., de Macedo, J. L., Dias, J. A., Dias, S. C., and Alvim, K. S. (2010). "Esterification of oleic acid with ethanol by 12-tungstophosphoric acid supported on zirconia," *Applied Catalysis A: General* 372(2), 153-161. DOI: 10.1016/j.apcata.2009.10.027

Pasquale, G., Vázquez, P., Romanelli, G., and Baronetti, G. (2012). "Catalytic upgrading of levulinic acid to ethyl levulinate using reusable silica-included Wells-Dawson heteropolyacid as catalyst," *Catalysis Communications* 18, 115-120. DOI: 10.1016/j.catcom.2011.12.004

Patel, A., and Brahmkhatri, V. (2013). "Kinetic study of oleic acid esterification over 12-tungstophosphoric acid catalyst anchored to different mesoporous silica supports," *Fuel Processing Technology* 113, 141-149. DOI: 10.1016/j.fuproc.2013.03.022

Rataboul, F., and Essayem, N. (2011). "Cellulose reactivity in supercritical methanol in the presence of solid acid catalysts: Direct synthesis of methyl-levulinate," *Industrial & Engineering Chemistry Research* 50(2), 799-805. DOI: 10.1021/ie101616e

Saka, S., and Kusdiana, D. (2001). "Biodiesel fuel from rapeseed oil as prepared in supercritical methanol," *Fuel* 80(2), 225-231. DOI: 10.1016/S0016-2361(00)00083-1

Sawai, O., Nunoura, T., and Yamamoto, K. (2013). "Reprint of: Application of subcritical water liquefaction as pretreatment for supercritical water gasification system in domestic waste water treatment plant," *The Journal of Supercritical Fluids* 79, 274-282. DOI: 10.1016/j.supflu.2013.04.012

Schwanninger, M., Rodrigues, J., Pereira, H., and Hinterstoisser, B. (2004). "Effects of short-time vibratory ball milling on the shape of FT-IR spectra of wood and cellulose," *Vibrational Spectroscopy* 36(1), 23-40. DOI: 10.1016/j.vibspec.2004.02.003

Tekin, K., Karagöz, S., and Bektaş, S. (2012). "Hydrothermal liquefaction of beech wood using a natural calcium borate mineral," *The Journal of Supercritical Fluids* 72, 134-139. DOI: 10.1016/j.supflu.2012.08.016

Tropecêlo, A., Casimiro, M., Fonseca, I., Ramos, A., Vital, J., and Castanheiro, J. (2010). "Esterification of free fatty acids to biodiesel over heteropolyacids immobilized on mesoporous silica," *Applied Catalysis A: General* 390(1), 183-189. DOI: 10.1016/j.apcata.2010.10.007

Warabi, Y., Kusdiana, D., and Saka, S. (2004). "Reactivity of triglycerides and fatty acids of rapeseed oil in supercritical alcohols," *Bioresource Technology* 91(3), 283-287. DOI: 10.1016/S0960-8524(03)00202-5

Xu, C., and Etcheverry, T. (2008). "Hydro-liquefaction of woody biomass in sub-and super-critical ethanol with iron-based catalysts," *Fuel* 87(3), 335-345. DOI: 10.1016/j.fuel.2007.05.013

Xu, J., Jiang, J., Dai, W., and Xu, Y. (2012). "Liquefaction of sawdust in hot compressed ethanol for the production of bio-oils," *Process Safety and Environmental Protection* 90(4), 333-338. DOI: 10.1016/j.psep.2012.01.001

Xu, Y., Zheng, X., Yu, H., and Hu, X. (2014). "Hydrothermal liquefaction of *Chlorella pyrenoidosa* for bio-oil production over Ce/HZSM-5," *Bioresource Technology* 156, 1-5. DOI: 10.1016/j.biortech.2014.01.010

Yamazaki, J., Minami, E., and Saka, S. (2006). "Liquefaction of beech wood in various supercritical alcohols," *Journal of Wood Science* 52(6), 527-532. DOI: 10.1007/s10086-005-0798-4

Zhao, Y.-p., Zhu, W.-w., Wei, X.-y., Fan, X., Cao, J.-p., Dou, Y.-q., Zong, Z.-m., and Zhao, W. (2013). "Synergic effect of methanol and water on pine liquefaction," *Bioresource Technology* 142, 504-509. DOI: 10.1016/j.biortech.2013.05.028

Article submitted: August 7, 2015; Peer review completed: September 20, 2015; Revised version received: September 24, 2015; Accepted: September 25, 2015; Published: October 2, 2015.
DOI: 10.15376/biores.10.4.7738-7751